Digest Journal of Nanomaterials and Biostructures Vol. 13, No. 2, April – June 2018, p. 519 - 526

DOES SINGLE CARBON NANOTUBE EFFECTS ON MECHANISM OF BIOTIN-STREPTAVIDIN BINDING? MOLECULAR DYNAMICS SIMULATION AND DENSITY FUNCTIONAL THEORY STUDY

O. SOLTANI, M. R. BOZORGMEHR*, M. MOMEN-HERAVI
Department of Chemistry, Mashhad Branch, Islamic Azad University, Mashhad, Iran

In this work molecular dynamics (MD) simulation along with density functional theory (DFT) was used to investigate changes in structure and dynamics of streptavidin-biotin complex due to presence of carbon nanotube (CNT). Two different MD simulations were performed involve streptavidin-biotin in absence and presence on CNT. From each simulation root-mean-square deviation (RMSD), root-mean-square fluctuation (RMSF), diffusion coefficient and contact map calculated for streptavidin. RMSD values revealed that dynamics of streptavidin is decrease in presence of CNT. Diffusion coefficient of protein in presence and absence of CNT are 0.0044×10^{-5} and 0.0248×10^{-5} $cm^2/_s$, respectively. The RMSF values displayed that flexibility of third and fifth beta sheets along with third loop of streptavidin are more decrease in presence of CNT. Fourteen residues of streptavidin have interactions with biotin (eight residues have hydrogen bond interaction and eight residues have hydrophobic interaction) in absence of CNT. However, eight residues of streptavidin have interactions with biotin in presence of CNT. Density functional results involve frontier orbitals and reduced density gradient (RDG) analysis were shown that reactivity of biotin in presence of CNT is increased. Also, hydrogen bond and steric interactions between biotin and streptavidin changes due to presence of CNT and van der Waals interaction has minor role in biotin-streptavidin interaction.

(Received January 20, 2018; Accepted May 31, 2018)

Keywords: Streptavidin-biotin, Diffusion coefficient, Hydrophobic interaction, Frontier orbital, Weak interactions

1. Introduction

Proteins Immobilization on carbon nanotubes (CNTs) has been pursued in the past [1-4]. The specific recognition properties coupled with the electronic properties of CNTs of the immobilized proteins would indeed make for an ideal miniaturized sensor [5, 6]. Development of chemical methods to immobilize protein molecules onto CNTs in a reliable manner is the important step in this area [5]. One of the ways to immobilize protein molecules onto CNTs is to adsorb streptavidin on CNTs presumably via hydrophobic interaction [5, 7]. Using streptavidin as a linker prevents nonspecific interactions of target molecules with CNTs [8]. The very strong non-covalent interaction between biotin and streptavidin is a common method to preparing single walled carbon nanotube (SWNT)-streptavidin complexes [9]. This method has been used in many cases for immobilization [10, 11]. Martinez *et al*. were used streptavidin as a linker between DNA and SWNT and prepare a biosensor for the optical and electronic detection of DNA hybridization. Their results showed that streptavidin prevents nonspecific interactions between DNA and CNT. Also, the wrapping of SWNT with streptavidin causes fluorescence and electrical detection of DNA hybridization [12]. Liu *et al*. prepared SWNT-streptavidin complex via biotin-streptavidin recognition that stable in 18 day and preserve strong biotin recognition capability. Their results showed that SWNT-streptavidin complex are useful for capturing and sensing biotinylated DNA [13]. The adsorption behavior of proteins on the sides of SWNTs was subject of the shim *et al*.

* Corresponding author: mr_bozorgmehr@yahoo.com

work. They showed non-covalent functionalization of SWNTs with surfactant and poly (ethylene glycol) resisting nonspecific adsorption of streptavidin [9].

Streptavidin is originating from the Streotomyces avidinii bacterium and its molecular weight is 66 kDa [14]. This protein is homo-tetramer and has an extraordinary high affinity for biotin [15]. The dissociation constant of biotin-streptavidin complex is on the order of$10^{-14}\,{}^{mol}/_{lit}$. This is one of the strongest non-covalent interactions known in nature [16]. There are a number of reasons for this remarkable affinity. The first reason is the very similarity of the molecular binding pocket and biotin. The second reason is extensive network of hydrogen bonds. Other interactions such as hydrophobic interaction of biotin with streptavidin residue especially tryptophan has important role to stability of biotin-streptavidin complex[17]. One biotin can bind to each monomer of streptavidin, thus a streptavidin protein has maximally four bounded biotin [18]. Biotin is an S-containing monocarboxylic acid with two heterocyclic rings fused together through one of their sides. Biotin has small size thus during conjugated with biological moieties for biochemical assays the activity of biological molecules will most likely unaffected [19]. Biotinylation of streptavidin can be help to isolate biological molecules from a sample by exploiting highly stable biotin-streptavidin complex. The immobilized streptavidin on CNTs should thus show biotin-binding properties. In fact during immobilization of streptavidin biotin binding site of protein should be face the aqueous phase and accessible for binding with biotinylated molecules [20]. Yang *et al*. designed a sensitive chemiluminescent immunoassay system based on an efficient streptavidin-functionalized CNTs platform. Their developed bio-functionalized-CNTs platform shows large reactive surface area and biocompatibility to capture biotinylated antibody [21].

In this manuscript, molecular dynamics simulation together with density functional theory was used to investigate biotin-streptavidin complex properties during interaction of streptavidin with single carbon nanotube.

2. Computational details

The crystal structure of streptavidin [PDB: 1STP] was retrieved from the Protein Data Bank [22].

Two simulation boxes with dimensions of $7 \times 7 \times 7\ nm^3$ were defined. Streptavidin was located in the center of the boxes. Then, SWNT molecule was placed randomly within the one of these boxes. Then simulation boxes were filled with TIP3P water [23]. In order to neutralize the systems, an appropriate number of Na^+ ions were added to each box. The OPLSAA force field was assigned for SWNT, biotin and protein. Since the parameters of the OPLSAA for SWNT and biotin have not been incorporated with GROMACS by default, these parameters were inserted manually. To do this, the geometry of SWNT was optimized using the Beck–Lee–Young–Parr exchange correlation functional (B3LYP) [24] as implemented in the Gaussian 03 program [25]. The 6-311+G (d, p) basis set was employed. The optimized geometry was confirmed to have no imaginary frequency of the Hessian. Optimized structure was visualized by using the Chemcraft 1.5 program [26]. To minimize the energy of the whole system and to relax the solvent molecules, the steepest descent algorithm was used. Further, to maintain equilibrium in the designed systems, simulation was performed for 1000 ps at NVT and NPT ensembles, respectively. Finally, each system was simulated with a time step of 2 fs for 30000 ps. The V-rescale coupling algorithm was employed to maintain various components at a constant temperature and pressure during simulations [27]. The PME algorithm [28] was used to determine the electrostatic interactions of each component of the systems. Covalent bonds present in the molecules were constrained using the LINCS algorithm [29] and the chemical bonds in solvent molecules were held constant using the SETTLE algorithm. All MD calculations were performed using the GROMACS 5.2.1. To investigate structure and electronic properties of biotin-streptavidin complex, average structure of biotin and its binding site was obtained from last nanosecond of each simulation and then the single-point energy calculations were performed at B3LYP/6-311+G(d, p) level of theory. The structure and electronic properties of this complex were analyzed by the Multiwfn software.

3. Results and discussions

In order to verify the equilibrium conditions of the systems, the RMSD values for each system were obtained using the following equation:

$$RMSD(t_1, t_2) = \left[\frac{1}{M}\sum_{i=1}^{N} m_i \|r_i(t_1) - r_i(t_2)\|^2\right]^{\frac{1}{2}} \quad (1)$$

where $M = \sum_{i=1}^{N} m_i$ and $r_i(t)$ is the position of atom i at time t. The RMSD changes over time are shown in Fig. 1.

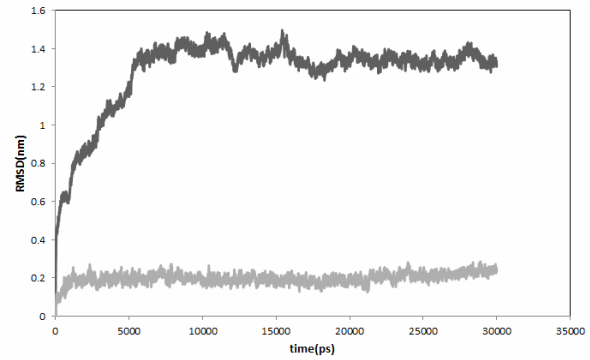

Fig. 1 The RMSD (nm) changes over time (ps). The bulk and bright curves are related to the streptavidin in the absence (STP) and presence (STP-SWNT) of the SWNT, respectively.

In this figure, the bulk and bright curves are related to the streptavidin in the absence (STP) and presence (STP-SWNT) of the SWNT, respectively. Regarding the figure, it can be seen that the protein has reached at equilibrium in the absence of the nanotube after 5000 ps while the protein in the presence of a nanotube is equilibrated in 1000 ps. Also, the amount of RMSD in the absence of nanotube is significantly lower than RMSD values in the presence of nanotubes. Therefore, it seems that the nanotube has reduced the protein's dynamics. For further investigation, the diffusion coefficient of the protein was calculated in two simulated systems. The prediction of the diffusion coefficients of molecules in water is of theoretical importance. As the diffusion coefficient value increases, the mobility of the molecule increases. Einstein relation was used to calculate diffusion coefficient of protein in two simulated systems:

$$D = \frac{1}{6}\lim_{t\to\infty}\frac{d}{dt}\langle|r_i(t) - r_i(0)|^2\rangle \quad (2)$$

where r_i is the atom coordinate vector and the term inside the angle brackets is the mean square displacement (MSD). In this approach, the self-diffusion coefficient (D) is proportional to the slope of the MSD as a function of time in the diffusional regime. The amount of protein diffusion coefficient in the presence and absence of nanotubes was calculated to be 0.0044×10^{-5} and $0.0248 \times 10^{-5}\frac{cm^2}{s}$, respectively. Thus, the nanotube has reduced the diffusion coefficient of the protein. This result is consistent with the values obtained for protein RMSDs.

Flexibility of streptavidin residues in the simulated systems is shown as RMSF (root mean square fluctuation) plot in Fig. 2.

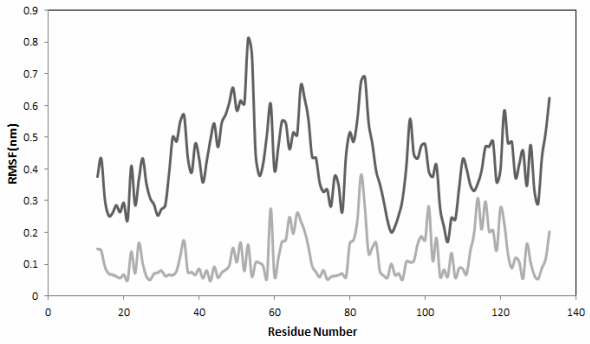

Fig. 2 Average root mean square fluctuation (RMSF) of residues of STP (bulk curve) and STP-SWNT (bright curve).

RMSF is considered as a scale of flexibility of the protein residues. According to this figure, it is observed that the flexibility of the protein residues in the presence of the nanotube has decreased. The pattern of the residues flexibility is different in simulations in two regions 38 to 50 and 71 to 79. The residues 38 to 50 are located on the third beta sheet and third loop of streptavidin. The residues of 38 to 50 are respectively Ala38, Leu39, Thr40, Gly41, Thr42, Tyr43, Glu44 (in third beta sheet) and Ser45, Ala46, Val47, Gly48, Asn49, Ala50 (in third loop). It can be seen that except for Glu44, the rest of the amino acids in this series are Hydrophobic. The residues 71 to 79 are located on the fifth beta sheet of streptavidin. The residues of 71 to 79 are respectively Thr71, Ala72, Leu73, Gly74, Trp75, Thr76, Val77, Ala78 and Trp79. All residues in this area are hydrophobic. Thus, Nanotubes interact with hydrophobic residues of streptavidin, in accordance with experimental results [21]. In Fig. 3, the average structure of streptavidin together with the SWNT is shown.

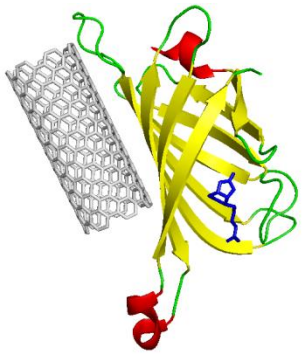

Fig. 3. Streptavidin average structure along with the SWNT. Biotin is shown in blue.

According to this figure it can be seen that the nanotube is located near the third and fifth beta-sheets. The streptavidin is partly flattened on the nanotube. The important point in this figure is that the nanotube has not blocked the beta barrel crater of streptavidin. Therefore, streptavidin can interact with biotinylated target molecules.

Fig. 4 shows the contact map (lower triangle) and the contact difference maps (upper triangle) of the structures of the streptavidin in presence and absence of SWNT obtained from the simulations.

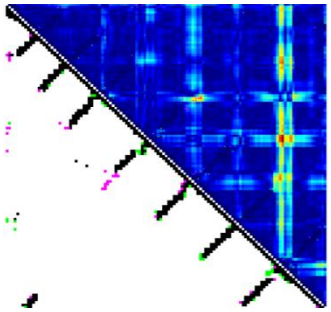

Fig. 4. The contact map (lower triangle) and the contact difference maps (upper triangle) of the structures of the streptavidin in presence and absence of SWNT obtained from the simulations. The colors used are described in the text.

In these figure, the black dots indicate the common contacts and the pink dots show the contacts that are present in the STP, but absent in the STP-SWNT. The green dots indicate the contacts that are present in the STP-SWNT, but absent in the STP. The differences between the structures are indicated by the intensity of the red and blue colors. The regions in blue color show the contacts that are not altered and those in the red color show the difference between the two structures. Some contacts that are different in the STP and STP-SWNT are: Tyr22…Leu25, Ala65…Ala72, Thr20…Val33 and Ser45…Asn49. All the different contacts between the STP and STP-SWNT are shown in Fig. 5.

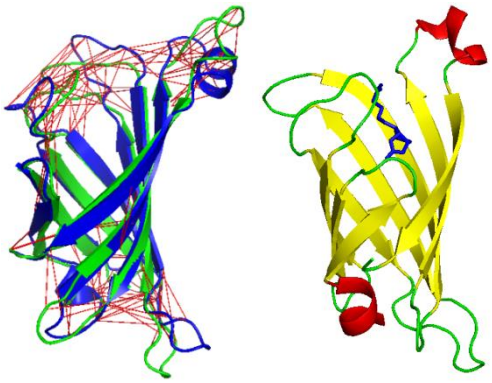

a) *b)*

Fig. 5. (a) all the different contacts between the STP and STP-SWNT are marked with red lines. The STP is shown in green and the STP-SWNT is shown in blue. In this figure, the STP is superimposed on the STP-SWNT;(b) The crystalline structure of the streptavidin is shown along with biotin (in blue color).

These contacts are marked with red lines. In this figure, the STP is shown in green and the STP-SWNT is shown in blue. In this figure, the STP is superimposed on the STP-SWNT. On the right side of this figure, the crystalline structure of the streptavidin is shown along with biotin (in blue color). It can be seen that the protein retains its own barrel structure during simulation. The crater of barrel for the STP-SWNT is tighter than the STP. This means that the ability to bind biotin to streptavidin changes in the presence of the nanotube. For further investigation, the biotin binding site of streptavidin was considered in the presence and absence of nanotubes. Figure 6 shows the biotin binding site for STP (left scheme) and STP-SWNT (right scheme). The following color scheme was used: Purple lines are ligand bonds; brown lines are non-ligand bond; green lines are hydrogen bonds and their length; red residues are non-ligand residues involved in hydrophobic contact(s).

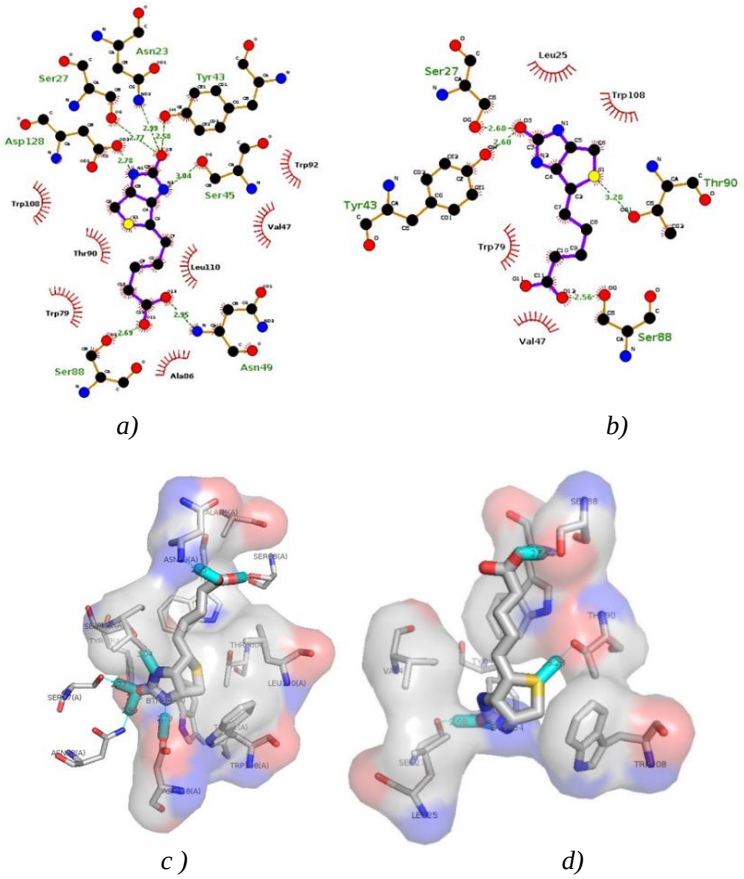

Fig. 6. a) the biotin binding site for STP. b) The biotin binding site for STP-SWNT. c) Three-dimensional shape of the biotin binding site for STP. d) Three-dimensional shape of the biotin binding site for STP-SWNT.

For STP, Val47, Trp79, Ala86, Thr90, Trp92, Trp108 and Leu110 residues are involved in hydrophobic contacts with the ligand and Asn23, Ser27, Tyr43, Ser45, Asn49, Ser88 and Asp128 residues interact with the ligand through hydrogen bonds. For the STP-SWNT, the number of residues in the binding site of biotin has decreased. For STP-SWNT, Leu25, Val47, Trp79 and Trp108 are involved in hydrophobic contacts with the ligand and ser27, Tyr43, Ser88 and Thr90 residues interact with the ligand through hydrogen bonds. Two new interactions (Leu25 and Thr90) have been created in presence of SWNT and six interactions remain intact, although the number of interactions has decreased from 16 to 8. These results indicate that the presence of nanotubes, in addition to changing the structure and dynamics of the streptavidin, also changes the binding affinity to the biotin. However, preserving the structure of the barrel and maintaining the network of hydrogen bond and hydrophobic interactions shows that biotin affinity to streptavidin is not too low. The three-dimensional shape of the biotin binding site is also shown in Fig. 6.

To determine the effect of nanotubes on biotin reactivity and its weak interactions, density functional theory was used. The frontier molecular orbital (FMO) theory, developed by Kenichi Fukui in 1950's is a practical model for describing chemical reactivity of chemical compounds [30]. In this theory, instead of considering the total electron density in a nucleophile site, we should consider the localization of the high occupied molecular orbital (HOMO) because electrons from these orbitals are most free to participate in the reaction. Also, FMO theory predicts that a good electrophilic site is a site where the lowest unoccupied molecular orbital (LUMO) is localized. The HOMO and LUMO orbitals of biotin were obtained in different simulations and are shown in Fig. 7.

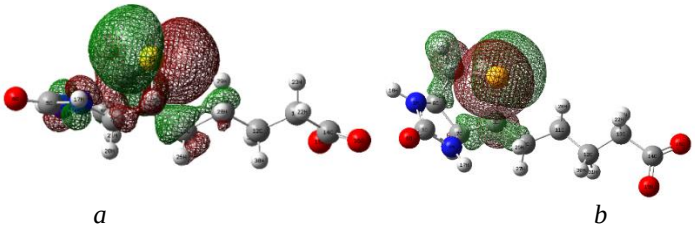

a *b*

Fig. 7. The frontier orbitals of biotin in (a) STP and (b) STP-SWNT.

According to the figure, the HOMO and LUMO orbital are localized on the biotin cyclic portion. Thus, the cyclic section of biotin is more reactive and will have a greater role in charge transfer. The energy difference of HOMO and LUMO orbitals for biotin in STP and STP-SWNT was obtained 0.05778 and 0.00684 (in atomic unit) respectively. As a result, nanotube has increased the reactivity of biotin. However, due to streptavidin deformation, the number of residues involved in the binding to biotin has decreased. Weak physical interaction has significant influence on binding mode of ligands to proteins and conformation of proteins [31, 32]. In Bader's QTAIM theory [33], that is widely used, in particular in the studies of ligand binding [32] by considering the products of $sign(\lambda_2)\rho(r)$ which λ_2 and ρ are second largest eigenvalue of Hessian matrix of electron density and electron density, respectively, one can not only know where weak interaction region is, but also know the interaction type. According to sign of λ_2 and ρ the following regions are defined:

Van der Waals interaction: $\rho \approx 0$ and $\lambda_2 \approx 0$.

Strong attraction: hydrogen bond and halogen bond: $\rho > 0$and$\lambda_2 < 0$.

Strong repulsion: steric effect in ring and cage.

The values of ρ and λ_2 calculated and results exhibited in Fig. 8 for biotin in STP and STP-SWNT interaction with its correspondence binding site residues, respectively.

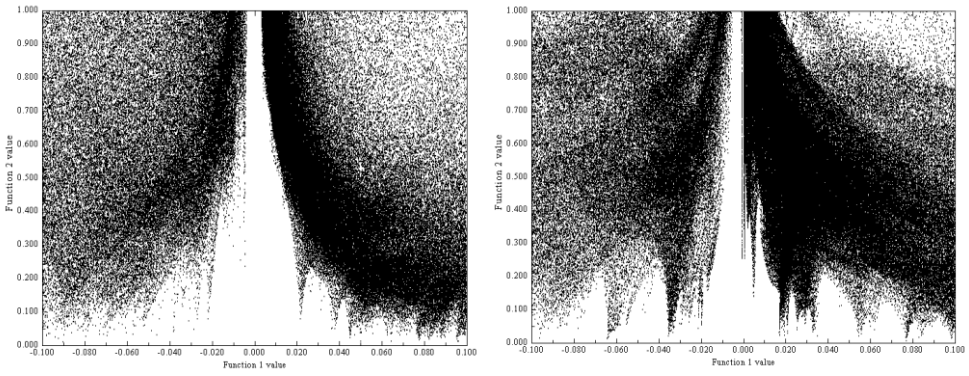

a) *b)*

Fig. 8. The weak interactions analysis of biotin in a) STP and b) STP-SWNT.

According to figures, the van der Waals interaction plays a small role in weak interactions, although its amount in the presence of the nanotubes has somewhat strengthened. In general, hydrogen bond and steric interactions play a significant role in both STP and STP-SWNT.

References

[1] W. Feng, P. Ji, Biotechnology Advances **29**(6), 889 (2011).
[2] S. Dharni et al., Journal of Biomolecular Structure and Dynamics **34**(1), 152 (2016).
[3] H. Zhou et al., Journal of Biomolecular Structure and Dynamics, 1 (2017).

[4] M. Tasviri et al., Progress in Reaction Kinetics and Mechanism **37**(2), 161 (2012).
[5] R. J. Chen et al., Journal of the American Chemical Society **123**(16), 3838 (2001).
[6] J. F. Liang, Y. T. Li, V. C. Yang, Journal of pharmaceutical sciences **89**(8), 979 (2000).
[7] F. Balavoine et al., Angewandte Chemie International Edition **38**(13/14), 1912 (1999).
[8] A. Arakaki et al., Biotechnology and bioengineering **88**(4), 543 (2004).
[9] M. Shim et al., Nano Letters **2**(4), 285 (2002).
[10] Y. Gao et al., Analytical Letters **42**(16), 2711 (2009).
[11] A. Erdem et al., Electroanalysis **22**(6), 611 (2010).
[12] M. T. Martínez et al., The Journal of Physical Chemistry C **116**(42), 22579 (2012).
[13] Z. Liu et al., The Journal of Physical Chemistry C **114**(10), 4345 (2010).
[14] J. Petrlova et al., Electroanalysis **19**(11), 1177 (2007).
[15] P. C. Weber et al., Journal of Biological Chemistry **262**(26), 12728 (1987).
[16] U. Piran, W. J. Riordan, Journal of immunological methods **133**(1), 141 (1990).
[17] H. Grubmüller, B. Heymann, P. Tavan, Science (5251), 997 (1996).
[18] M. Howarth et al., Nature methods **3**(4), 267 (2006).
[19] K. J. Roux et al., J. Cell Biol. **196**(6), 801 (2012).
[20] J. D. Hirsch et al., Analytical biochemistry **308**(2), 343 (2002).
[21] Z. Yang et al., Analytica chimica acta **774**, 85 (2013).
[22] P. C. Weber et al., Science **243**(4887), 85 (1989).
[23] W. L. Jorgensen et al., The Journal of chemical physics **79**(2), 926 (1983).
[24] R. G. Parr, W. Yang, Journal of the American Chemical Society **106**(14), 4049 (1984).
[25] M. Frisch, Gaussian 03, Revision B. 05 and D. 01, Gaussian. Inc., Pittsburgh PA, 2003.
[26] G. Zhurko, D. Zhurko, Chemcraft program, Academic version 1.5,(2004). Available on line www. Chemcraftprogram. com, 2004.
[27] G. Bussi, D. Donadio, M. Parrinello, The Journal of chemical physics **126**(1), 014101 (2007).
[28] T. Darden, D. York, L. Pedersen, The Journal of chemical physics **98**(12), 10089 (1993).
[29] B. Hess et al., Journal of computational chemistry **18**(12), 1463 (1997).
[30] K. Fukui, T. Yonezawa, H. Shingu, The Journal of Chemical Physics **20**(4), 722 (1952).
[31] C. V. Robinson et al., Journal of the American Chemical Society **118**(36), 8646 (1996).
[32] M. R. Bozorgmehr, J. Chamani, G. Moslehi, Journal of Biomolecular Structure and Dynamics **33**(8), 1669 (2015).
[33] J. Cioslowski, Science **252**(5012), 1566 (1991).